An energy harvesting technology controlled by ferromagnetic resonance

Cite as: AIP Advances **11**, 085114 (2021); https://doi.org/10.1063/5.0056724
Submitted: 01 June 2021 • Accepted: 28 July 2021 • Published Online: 10 August 2021

Yuta Nogi, Yoshio Teki and Eiji Shikoh

An energy harvesting technology controlled by ferromagnetic resonance

Cite as: AIP Advances 11, 085114 (2021); doi: 10.1063/5.0056724
Submitted: 1 June 2021 • Accepted: 28 July 2021 •
Published Online: 10 August 2021

Yuta Nogi,[1] Yoshio Teki,[2] and Eiji Shikoh[1,a)]

AFFILIATIONS

[1] Graduate School of Engineering, Osaka City University, 3-3-138 Sugimoto, Sumiyoshi-ku, Osaka 558-8585, Japan
[2] Graduate School of Science, Osaka City University, 3-3-138 Sugimoto, Sumiyoshi-ku, Osaka 558-8585, Japan

[a)] **Author to whom correspondence should be addressed:** shikoh@eng.osaka-cu.ac.jp

ABSTRACT

We have successfully demonstrated electrical charging using the electromotive force (EMF) generated in a ferromagnetic metal (FM) film under ferromagnetic resonance (FMR). In the case of $Ni_{80}Fe_{20}$ films, electrical charge due to the EMF generated under FMR can be accumulated in a capacitor; however, the amount of charge is saturated well below the charging limit of the capacitor. Meanwhile, in the case of $Co_{50}Fe_{50}$, electrical charge generated under FMR can be accumulated in a capacitor and the amount of charge increases linearly with the FMR duration time. The difference between the $Ni_{80}Fe_{20}$ and $Co_{50}Fe_{50}$ films is due to the respective magnetic field ranges for the FMR excitation. When the FM films were in equivalent thermal states during FMR experiments, $Co_{50}Fe_{50}$ films could maintain FMR in a detuned condition, while $Ni_{80}Fe_{20}$ films were outside the FMR excitation range. The EMF generation phenomenon in an FM film under FMR can be used as an energy harvesting technology by appropriately controlling the thermal conditions of the FM film.

Energy harvesting is an important technology to efficiently utilize the Earth's natural resources.[1] This technology harvests the existing micro-energy in an environment and is different from conventional electric generation technologies, such as electric power plants. So far, the harvesting of such micro-energies has focused on the use of light, heat, vibration, electromagnetic fields, and their related phenomena.[1] The energy obtained per system due to such harvesting methods is not very large; however, the harvested electric power has the potential to be used to operate electronic devices.

Ferromagnetic resonance (FMR) is a magnetic phenomenon in which the magnetization dynamics in a magnetic material is controlled using both a static magnetic field (H) and a high frequency magnetic field in the GHz band.[2] From research on spintronics, it has been discovered that an electromotive force (EMF) is generated in the ferromagnetic metal (FM) film itself under FMR.[3,4] The EMF originates from various physical phenomena, such as the inverse spin-Hall effect (ISHE)[3–5] and the anomalous Hall effect (AHE).[3–5] In conventional devices, the EMF generated in the FM film under FMR must be carefully removed, for example, in spin injection and spin transport experiments by the spin-pumping driven by the FMR.[5–14] Meanwhile, the EMF generation phenomenon itself in an FM film under FMR is the focus of this study, independent of the EMF origins. We have conceived an energy harvesting technology that uses this EMF generation phenomenon under FMR. This has a certain advantage, that is, the EMF in an FM film under FMR can be generated with all microwave with various frequency ranges existing in the environment, as long as the FMR condition is satisfied. In this concept, while the output voltage per FM film is much small, if it is possible to catch a microwave energy through the FMR excitation and to use a series connection consisting of various FM films with different FMR conditions, in principle, the EMF can be generated in all frequency ranges of microwaves because this generated EMF under FMR is a DC voltage. While the absolute value of the instant output voltage per FM film is small (approximately several μV),[3,4] we have conceived to use this EMF phenomenon as a battery at emergency by keeping the FMR almost permanently for charging. In this study, we have successfully demonstrated electrical charging using the EMF generated in an FM film itself under the FMR and show that the EMF generation phenomenon under the FMR is usable as an energy harvesting technology with appropriate control of the thermal conditions of the FM film.

Figure 1(a) shows a schematic illustration of our sample structure and the experimental setup to detect the EMF generated in the sample under FMR. An FM film was formed on a thermally

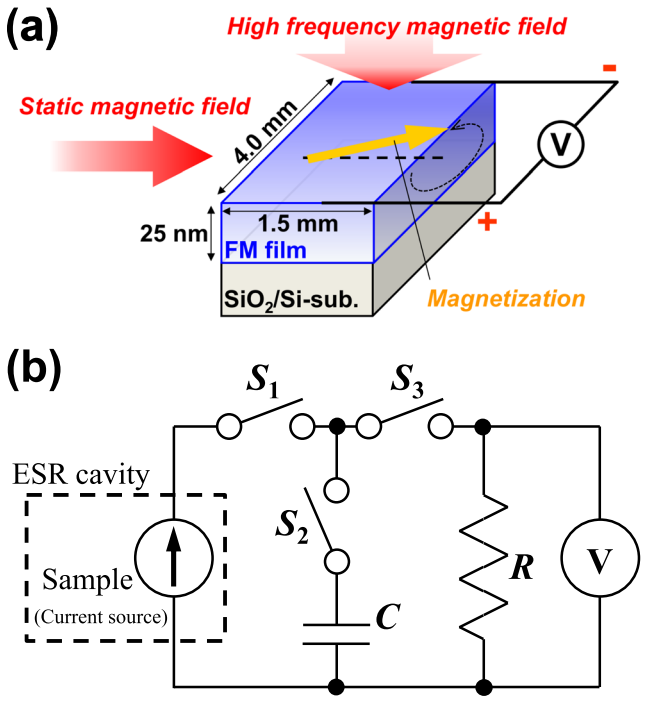

FIG. 1. (a) A schematic illustration of our sample structure and the experimental setup to detect the EMF generated in the sample under FMR. (b) Electrical circuit to evaluate the electric charging properties.

oxidized silicon substrate using an electron beam deposition system at pressure $<10^{-6}$ Pa. $Ni_{80}Fe_{20}$ (Kojundo Chemical Laboratory Co., Ltd., 99.99% purity) or $Co_{50}Fe_{50}$ (Kojundo Chemical Laboratory Co., Ltd., 99.99%) was used as the FM film. The deposition rate and the substrate temperature during FM deposition were set to 0.03 nm/s and room temperature (RT), respectively. No cover layer to prevent the FM films from oxidizing was formed because only the EMF phenomenon generated in the FM films under the FMR was considered in this study, not the individual origins of EMFs. After the FM deposition, the sample substrates were cut to the designed size, as shown in Fig. 1(a).

To confirm the EMF properties generated in the FM films under FMR, a microwave TE_{011}-mode cavity in an electron spin resonance system (JEOL, JES-TE300) was used to excite the FMR in an FM film, and a nanovoltmeter (Keithley Instruments, 2182A) was used to measure the EMF. Lead wires to detect the output voltage properties were directly attached at both ends of the FM film with silver paste.

To evaluate the electric charging properties under the FMR, the electrical circuit shown in Fig. 1(b) was connected to the FM film sample, in place of the nanovoltmeter used for the above EMF confirmation. First, all of the switches S_1, S_2, and S_3 were opened and the capacitor (the capacitance is C) was completely discharged. In the case of charging experiments, S_1 and S_2 are closed and the FMR of the FM film was excited by the same ESR system as described above. The electrical current derived from the EMF generated in the FM film under the FMR flowed and the electric charges were accumulated in the capacitor for the FMR duration time. The FMR condition in an in-plane field was set according to Kittel's formula[15]

$$\frac{\omega}{\gamma} = \sqrt{H_{FMR}(H_{FMR} + 4\pi M_S)}, \quad (1)$$

where ω, γ, H_{FMR}, and M_S are the angular frequency ($2\pi f$), the gyromagnetic ratios of 1.86×10^7 G^{-1} s^{-1} for $Ni_{80}Fe_{20}$[2,8] and 1.84×10^7 G^{-1} s^{-1} for $Co_{50}Fe_{50}$ calculated from the g-factor,[16] the FMR field, and the saturation magnetization of the FM film, respectively. After the charging processes, both S_1 and S_2 were opened.

Next, the accumulated charges in the capacitor were discharged using a so-called RC-series circuit, where the accumulated charges in the capacitor are consumed in a resistor (the resistance is R) as heat. Before starting discharge experiments for evaluation of the amount of charge accumulated in the charging processes, S_3 was closed, that is, the same nanovoltmeter as above was connected. The trigger for discharge is S_2. When S_2 is closed, an electric current due to the charge accumulated in the C starts to flow and is consumed at the resistor. In the RC-series circuit shown in Fig. 1(b), the electrical voltage between the terminals of the resistor is defined as $V(t)$, which is described by the following equation:

$$V(t) = V_0 \exp\left(-\frac{t}{\tau}\right), \quad (2)$$

where V_0, t, and τ are the initial voltage corresponding to the accumulated charge during the FMR duration time, the duration time from the trigger of the discharge process, and the time constant of the discharge circuit, which is defined as RC. In this study, τ was always set to be 1 s for ease of measurement (for example, R:C = 1 Ω:1 F). All evaluations were performed at RT.

Figures 2(a) and 2(b) show the FMR spectrum of an $Ni_{80}Fe_{20}$ film and the EMF generated in the same $Ni_{80}Fe_{20}$ film itself under the FMR at the microwave frequency and a power (P) of 9.45 GHz and 200 mW, respectively. In Fig. 2(b), the circles represent experimental data and the solid line is the fitted curve obtained using the following equation:[3–5,8–14]

$$V(H) = V_{Sym}\frac{\Gamma^2}{(H - H_{FMR})^2 + \Gamma^2} + V_{Asym}\frac{-2\Gamma(H - H_{FMR})}{(H - H_{FMR})^2 + \Gamma^2}, \quad (3)$$

where Γ denotes the fitting parameter including the intrinsic Gilbert damping or magnetic inhomogeneities (26 Oe for $Ni_{80}Fe_{20}$ in this study). The first and second terms in Eq. (3) correspond to the symmetry term for H due to the ISHE and the asymmetry term for H due to the AHE and/or other effects showing the same asymmetric voltage behavior relative to H, respectively.[3–5,8–14] V_{Sym} and V_{Asym} correspond to the coefficients of the first and second terms in Eq. (3). The H_{FMR} of the $Ni_{80}Fe_{20}$ film was 1100 Oe and the M_S of the $Ni_{80}Fe_{20}$ film was estimated to be 646 emu/cc with Eq. (1). The output voltages from the $Ni_{80}Fe_{20}$ film under the FMR are observed at H_{FMR}. The observed EMF is mainly due to the self-induced ISHE in the $Ni_{80}Fe_{20}$ film under FMR.[3]

Figures 2(c) and 2(d) show the FMR spectrum of a $Co_{50}Fe_{50}$ film and the EMF generated in the same $Co_{50}Fe_{50}$ film itself under the FMR at the microwave frequency and a P of 9.45 GHz and 200 mW, respectively. In Fig. 2(d), the circles represent experimental data and the solid line is the fitted curve obtained using Eq. (3) with the Γ of 110 Oe for $Co_{50}Fe_{50}$ in this study. The H_{FMR} of the

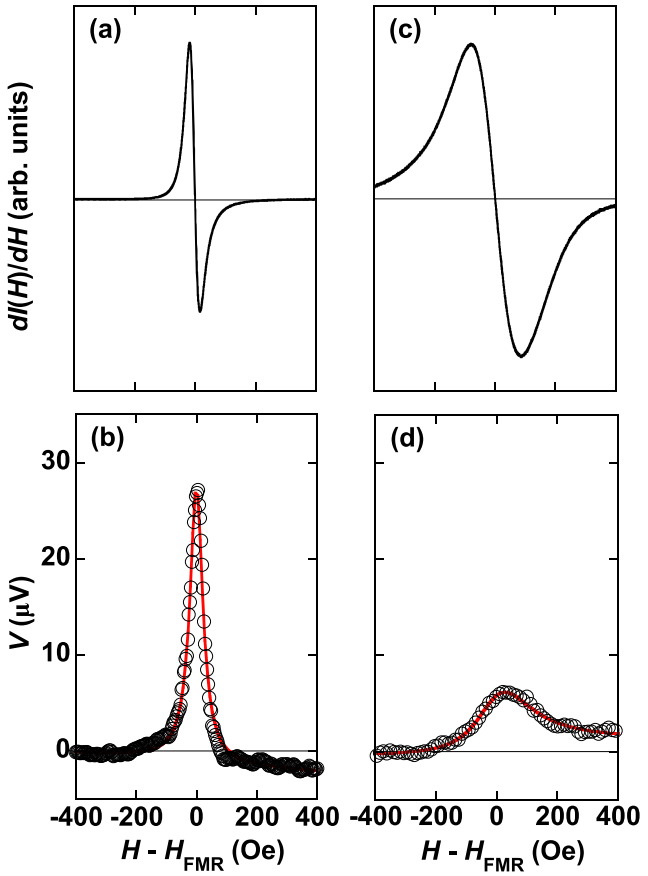

FIG. 2. (a) FMR spectrum of a $Ni_{80}Fe_{20}$ film and (b) the EMF generated in the same $Ni_{80}Fe_{20}$ film under FMR. (c) FMR spectrum of a $Co_{50}Fe_{50}$ film and (d) the EMF generated in the same $Co_{50}Fe_{50}$ film under FMR. The microwave frequency and power are 9.4 GHz and 200 mW, respectively.

$Co_{50}Fe_{50}$ film was 572 Oe and the M_S of the $Co_{50}Fe_{50}$ film was estimated to be 1410 emu/cc with Eq. (1). The FMR spectrum of the $Co_{50}Fe_{50}$ film is wider than that of the $Ni_{80}Fe_{20}$ film, corresponding to the difference in the damping constants of the materials and/or distinct structural/magnetic inhomogeneities resulting in spatial fluctuations of magnetic anisotropy. Output voltages from the $Co_{50}Fe_{50}$ film under the FMR are observed at H_{FMR}. The origins of the EMF generated in a $Co_{50}Fe_{50}$ film under FMR are currently under investigation,[17] while these might come from the ISHE, the AHE, and so on, similar to other FM films, such as $Ni_{80}Fe_{20}$, Fe, and Co films.[3,4] While the apparent EMF generated in the $Co_{50}Fe_{50}$ film at the H_{FMR} is smaller than that of the $Ni_{80}Fe_{20}$ film, it is sufficient for the energy-harvesting experiments in this study.

The energy-harvesting experiments are described below. First, using the charging circuit, the electric current generated in the FM films under the respective FMR condition to satisfy Eq. (1) flows and the capacitor is charged. The microwave power was 200 mW in all experiments except for the evaluation of *P*-dependence. Each FMR excitation was maintained for 30 min with the FMR condition to satisfy Eq. (1), and then, the capacitor was discharged. Figure 3(a) shows typical discharge properties of the capacitor evaluated using

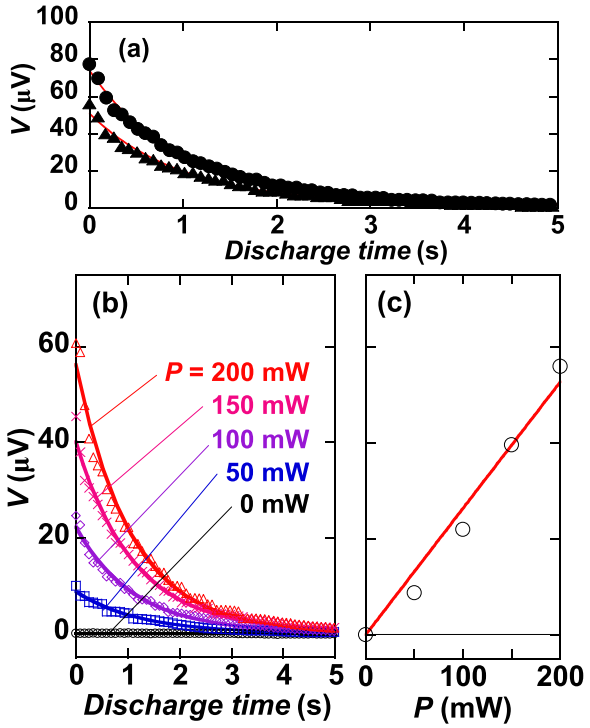

FIG. 3. (a) Typical discharge properties of capacitors evaluated using the discharge circuit. Circles and triangles are experimental data for a $Ni_{80}Fe_{20}$ film and a $Co_{50}Fe_{50}$ film, respectively. (b) Microwave power (*P*) dependences of discharge properties for a $Ni_{80}Fe_{20}$ film. Each FMR duration time (the charging time) was 30 min. The solid lines are fitted curves obtained using Eq. (2). (c) The *P*-dependence of the V_0 obtained by analysis of (b).

the discharge circuit. Circles and triangles are experimental data for a $Ni_{80}Fe_{20}$ film and a $Co_{50}Fe_{50}$ film, respectively. The solid lines are fitted curves obtained using Eq. (2), and the respective data showed a good fit. The V_0 is about 78 μV for the $Ni_{80}Fe_{20}$ film and 56 μV for the $Co_{50}Fe_{50}$ film. Figure 3(b) shows the *P*-dependences of the discharge properties for a $Ni_{80}Fe_{20}$ film. In this case, also, each FMR duration time (the charging time) was 30 min. The solid lines are also fitted curves obtained using Eq. (2). Figure 3(c) shows the *P*-dependence of the V_0 analyzed from Fig. 3(b). The value of V_0 increases linearly with the increase in *P*, that is, the charging is clearly due to the FMR phenomena.

Figure 4 shows the FMR duration time dependence of the discharge properties of a $Ni_{80}Fe_{20}$ film. The solid lines are fitted curves obtained using Eq. (2). Figure 4(b) shows the FMR duration time dependence of the V_0 generated in the $Ni_{80}Fe_{20}$ film from analysis of Fig. 4(a). The amount of charge from the $Ni_{80}Fe_{20}$ film tends to be saturated well below the voltage limit of the capacitor when the FMR duration time is over 15 min. To investigate the reason why the charge is saturated, we changed the capacitors and resistors while keeping τ at 1 s. In addition, other $Ni_{80}Fe_{20}$ films were tested. However, in all harvesting experiments with $Ni_{80}Fe_{20}$ films, the charge was saturated against the FMR duration time. Therefore, we changed the FM film from $Ni_{80}Fe_{20}$ to another FM.

Figure 5 shows the FMR duration time dependence of the discharge properties of a $Co_{50}Fe_{50}$ film. The solid lines are fitted curves

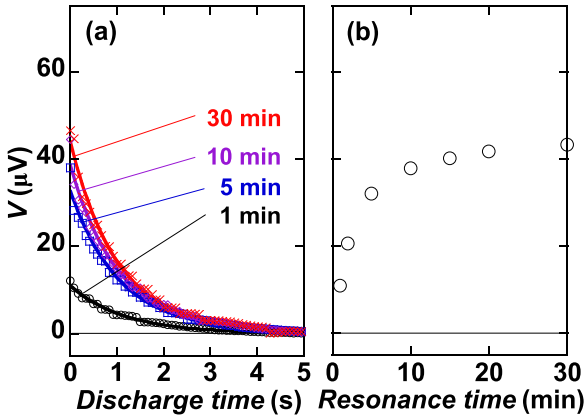

FIG. 4. (a) FMR duration time dependence of the discharge properties of a $Ni_{80}Fe_{20}$ film. The solid lines are fitted curves obtained using Eq. (2). (b) The FMR duration time dependence of the V_0 generated in the $Ni_{80}Fe_{20}$ film from analysis of (a).

obtained using Eq. (2). Figure 5(b) shows the FMR duration time dependence of the V_0 generated in the $Co_{50}Fe_{50}$ film obtained by analysis of Fig. 5(a). The amount of charge from the $Co_{50}Fe_{50}$ film increases almost linearly with increasing FMR duration time and is not saturated. This behavior is different from the case of the $Ni_{80}Fe_{20}$ film shown in Fig. 4(b), and this characteristic shows good reproducibility with other $Co_{50}Fe_{50}$ films. It is noticed that while the apparent EMF generated in the $Co_{50}Fe_{50}$ film at the H_{FMR} is smaller than that in the $Ni_{80}Fe_{20}$ film, the FMR spectrum of a $Co_{50}Fe_{50}$ film is much wider than that of a $Ni_{80}Fe_{20}$ film. The FM film under FMR is basically heated. Notably, the FMR duration time in this study is very long compared with general FMR experiments. The M_S of an FM film becomes smaller at a high temperature than at a low temperature. That is, in the case of the in-plane magnetic field, as shown in Eq. (1), the H_{FMR} of an FM film becomes larger at a high

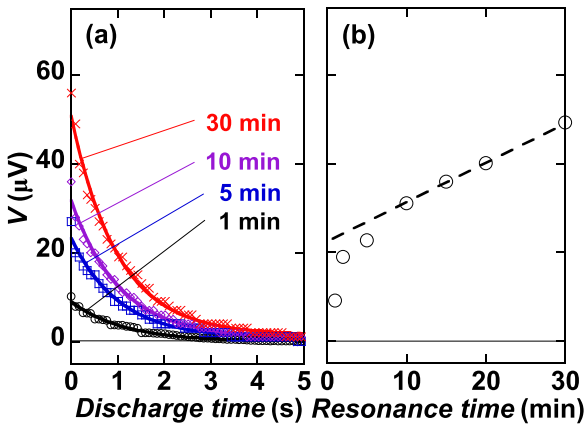

FIG. 5. (a) FMR duration time dependence of the discharge properties of a $Co_{50}Fe_{50}$ film. The solid lines are fitted curves obtained using Eq. (2). (b) The FMR duration time dependence of V_0 generated in the $Co_{50}Fe_{50}$ film from analysis of the data in (a). The dashed line is a guide for the eyes.

temperature than at a low temperature when the microwave frequency is the same. Thus, in the experiments with $Ni_{80}Fe_{20}$ films, the film was heated and the H_{FMR} shifted to larger values compared with the beginning of the experiment. Because the ESR-system parameters were kept the same in the experiments, the $Ni_{80}Fe_{20}$ film might have gone out of the FMR excitation range. Therefore, EMF was hardly generated and the charging of the capacitor almost stopped. Meanwhile, in the experiments with $Co_{50}Fe_{50}$ films, the film was heated under the FMR and the H_{FMR} also became larger compared with the beginning of the experiment. Similarly, the ESR-system settings were maintained in the experiments. However, the $Co_{50}Fe_{50}$ film might not be fully out of the FMR excitation range for $Co_{50}Fe_{50}$ films due to the wider FMR spectrum than $Ni_{80}Fe_{20}$. Therefore, the EMF generation in $Co_{50}Fe_{50}$ films under FMR was kept in a detuned state and the charging to the capacitor was maintained. Of course, thermally equivalent conditions for similar experiments must depend on the microwave cavity used and other thermal factors. That is, by appropriately controlling the thermal conditions around the FM film, the charging was maintained. The above result indicates that energy-harvesting experiments using FMR were successfully demonstrated.

At present, no diodes were connected to the circuit to rectify the electrical currents. To efficiently charge the capacitor and to increase the amount of accumulated charge, the use of diodes may be effective because the currents generated by an FM film under the FMR are very small and controlling the flow of such micro-currents is usually difficult. The microwave power was kept the same (200 mW) in all experiments except for the evaluation of P-dependence. A smaller microwave power may be preferable to reduce heating of the films and to precisely control the thermal conditions of the FM film under FMR. For controlling FMR with a good thermal condition, the use of an FM film with a higher Curie temperature (T_C) is better because the M_S of the FM film is not so changed against the environmental temperature change. In this sense, it is reasonable that a $Co_{50}Fe_{50}$ film shows better performance than $Ni_{80}Fe_{20}$ because T_C of $Co_{50}Fe_{50}$ is much higher than $Ni_{80}Fe_{20}$. It would also be effective to set the static magnetic field in expectation of temperature increase, for example, in an in-plane field case, the static magnetic field should be set a little bit higher than an usual FMR field, within the possible FMR range. In general, a large electric power is required to apply the electric current to provide a static magnetic field and a high frequency field. Thus, methods should be developed to reduce the electric power required for the excitation of FMR, for example, using permanent magnets to create the static magnetic field and environmental electromagnetic waves for a high frequency magnetic field. According to the previous $Ni_{80}Fe_{20}$ case,[3] the EMF can be generated in almost all orientation of the static magnetic field except for completely perpendicular to the film plane. To prepare a uniform magnetic field with permanent magnets for FMR excitation, the use of an almost perpendicular magnetic field to the FM film plane would be easier than an in-plane field. While those might be hard to be established, such technology is eagerly awaited because a lot of GHz-band microwaves exist in modern environments, such as those used in wireless internet services. The above issues must be solved for practical use. Our target may be close to other research for low grade energy from the environment to power low-power devices on energy harvesting.[18–20] As long as the FMR condition is satisfied, in principle, the EMF continues to be generated in FM films

in all frequency ranges of the RF magnetic field. Thus, by using a series-connecting electric circuit consisting of FM films with various M_S, frequency-variable EMF generation by using FMR will be possible. This is an advantage on our concept to others.[18–20] Because the instantly obtained EMF per FM film is tiny in this study (approximately several μV), by keeping the FMR for charging, it would be necessary for ~15 000 h (over 600 days) to obtain 1.5 V, which is a typical value of general dry cells. However, because the EMF generated in this study is a DC voltage, in a case with 20 pieces of the same FM films with a series connection, the charging time for 1.5 V would be estimated to reduce to about one month. For practical use, a storage battery instead of a capacitor should be used for preventing from quickly running out.

In summary, we successfully demonstrated electrical charging using the EMF generated in a FM film under FMR. In the case of $Ni_{80}Fe_{20}$, electrical charge due to the EMF generated under the FMR was stored in a capacitor; however, the amount of charge was saturated well below the charging limit of the capacitor despite the increase in FMR duration time. Meanwhile, in the case of $Co_{50}Fe_{50}$, electrical charge generated under the FMR was stored in a capacitor and the amount of charge increased linearly with the FMR duration time. The FMR spectrum of the $Co_{50}Fe_{50}$ films was wider than that of $Ni_{80}Fe_{20}$. In equivalent thermal states, during FMR experiments, $Co_{50}Fe_{50}$ films maintained FMR in a detuned condition, while $Ni_{80}Fe_{20}$ films were outside of the FMR excitation range. The above result indicated that the EMF generation phenomenon in FM films under FMR might be usable as an energy harvesting technology by appropriately controlling the thermal conditions of the FM films.

AUTHORS' CONTRIBUTIONS

E.S. conducted the study. Y.N. carried out all experiments. Y.T. set up the ESR system. Y.N. and E.S. analyzed the experimental results. All authors contributed to writing and discussions about this manuscript.

This research was partly supported by a research grant from the Murata Science Foundation and a research grant from the Mazda Foundation.

DATA AVAILABILITY

The data that support the findings of this study are available from the corresponding author upon reasonable request.

REFERENCES

[1] H. Akinaga, H. Fujita, M. Mizuguchi, and T. Mori, Sci. Technol. Adv. Mater. **19**, 543 (2018).
[2] C. Kittel, *Introduction to Solid State Physics*, 8th ed. (Wiley, 2004).
[3] A. Tsukahara, Y. Ando, Y. Kitamura, H. Emoto, E. Shikoh, M. P. Delmo, T. Shinjo, and M. Shiraishi, Phys. Rev. B **89**, 235317 (2014).
[4] K. Kanagawa, Y. Teki, and E. Shikoh, AIP Adv. **8**, 055910 (2018).
[5] E. Saitoh, M. Ueda, H. Miyajima, and G. Tatara, Appl. Phys. Lett. **88**, 182509 (2006).
[6] S. Mizukami, Y. Ando, and T. Miyazaki, Phys. Rev. B **66**, 104413 (2002).
[7] Y. Tserkovnyak, A. Brataas, and G. E. W. Bauer, Phys. Rev. Lett. **88**, 117601 (2001).
[8] K. Ando and E. Saitoh, J. Appl. Phys. **108**, 113925 (2010).
[9] E. Shikoh, K. Ando, K. Kubo, E. Saitoh, T. Shinjo, and M. Shiraishi, Phys. Rev. Lett. **110**, 127201 (2013).
[10] Y. Tani, Y. Teki, and E. Shikoh, Appl. Phys. Lett. **107**, 242406 (2015).
[11] Y. Tani, T. Kondo, Y. Teki, and E. Shikoh, Appl. Phys. Lett. **110**, 032403 (2017).
[12] Y. Tanaka, T. Kono, Y. Teki, and E. Shikoh, IEEE Trans. Magn. **55**, 1400304 (2019).
[13] K. Nishida, Y. Teki, and E. Shikoh, Solid State Commun. **312**, 113898 (2020).
[14] K. Tamura, T. Kanki, S. Shirai, H. Tanaka, Y. Teki, and E. Shikoh, AIP Adv. **11**, 035120 (2021).
[15] C. Kittel, Phys. Rev. **73**, 155 (1948).
[16] F. Schreiber, J. Pflaum, Z. Frait, Th. Mühge, and J. Pelzl, Solid State Commun. **93**, 965 (1995).
[17] S. Baek, Y. Teki, and E. Shikoh, "Composition dependence of the self-induced inverse spin-Hall effect in Co-Fe alloy single-layer films under their ferromagnetic resonance" (unpublished).
[18] J. P. G. Tarelho, M. P. Soares dos Santos, J. A. F. Ferreira, A. Ramos, S. Kopyl, S. O. Kim, S. Hong, and A. Kholkin, Mater. Today **21**, 1019 (2018).
[19] V. Annapureddy, H. Palneedi, G.-T. Hwang, M. Peddigari, D.-Y. Jeong, W.-H. Yoon, K.-H. Kim, and J. Ryu, Sustainable Energy Fuels **1**, 2039 (2017).
[20] J. V. Vidal, A. V. Turutin, I. V. Kubasov, A. M. Kislyuk, D. A. Kiselev, M. D. Malinkovich, Y. N. Parkhomenko, S. P. Kobeleva, N. A. Sobolev, and A. L. Kholkin, IEEE Trans. Ultrason., Ferroelectr., Freq. Control **67**, 1219 (2020).